Host Adaptation in *Legionellales* Is 1.9 Ga, Coincident with Eukaryogenesis

Eric Hugoson,[†,1,2] Andrei Guliaev,[†,1] Tea Ammunét,[‡,1] and Lionel Guy [iD][*,1]

[1]Department of Medical Biochemistry and Microbiology, Science for Life Laboratories, Uppsala University, Uppsala, Sweden
[2]Department of Microbial Population Biology, Max Planck Institute for Evolutionary Biology, Plön, Germany

***Corresponding author:** E-mail: lionel.guy@imbim.uu.se.
[†]These authors contributed equally to this work.
[‡]Present address: Medical Bioinformatics Centre, Turku Bioscience, University of Turku, Turku, Finland
Associate editor: Heather Hendrickson

Abstract

Bacteria adapting to living in a host cell caused the most salient events in the evolution of eukaryotes, namely the seminal fusion with an archaeon, and the emergence of both mitochondrion and chloroplast. A bacterial clade that may hold the key to understanding these events is the deep-branching gammaproteobacterial order *Legionellales*—containing among others *Coxiella* and *Legionella*—of which all known members grow inside eukaryotic cells. Here, by analyzing 35 novel *Legionellales* genomes mainly acquired through metagenomics, we show that this group is much more diverse than previously thought, and that key host-adaptation events took place very early in its evolution. Crucial virulence factors like the Type IVB secretion (Dot/Icm) system and two shared effector proteins were gained in the last *Legionellales* common ancestor (LLCA). Many metabolic gene families were lost in LLCA and its immediate descendants, including functions directly and indirectly related to molybdenum metabolism. On the other hand, genome sizes increased in the ancestors of the *Legionella* genus. We estimate that LLCA lived approximately 1.89 Ga, probably predating the last eukaryotic common ancestor by approximately 0.4–1.0 Gy. These elements strongly indicate that host adaptation arose only once in *Legionellales*, and that these bacteria were using advanced molecular machinery to exploit and manipulate host cells early in eukaryogenesis.

Key words: Legionella, eukaryogenesis, phlyogenomics, metagenomics, host adaptation.

Introduction

The recent discovery of Asgard archaea and their placement on the tree of life (Spang et al. 2015; Zaremba-Niedzwiedzka et al. 2017) sheds light on early eukaryogenesis, confirming that eukaryotes arose from a fusion between an archaeon and a bacterium. However, many questions pertaining to eukaryogenesis remain unanswered. In particular, the timing and the nature of the fusion are vigorously debated (Poole and Gribaldo 2014; Pittis and Gabaldón 2016; Eme et al. 2017; López-García et al. 2017). Mito-late scenarios (López-García and Moreira 2006; Pittis and Gabaldón 2016; Spang et al. 2019) posit that endosymbiosis of the mitochondrion occurred in a eukaryote that was capable of phagocytosis, whereas mito-early scenarios (Martin and Müller 1998; Martin et al. 2017) posit that mitochondrial endosymbiosis triggered eukaryogenesis. A recent study proposed a "mito-intermediate" scenario, where the pre-endosymbiosis eukaryote was somewhat complex, with a dynamic cytoskeleton and a membrane trafficking system, but the endomembrane system, and the transcription regulation and signaling systems occurred postendosymbiosis (Vosseberg et al. 2021). In many scenarios including the latter, phagocytosis is

considered a prerequisite for mitochondrion endosymbiosis and therefore a key component needed for eukaryogenesis (Poole and Gribaldo 2014). It is not certain when eukaryotes gained the ability to phagocytose bacteria, but it was most certainly prior to the last eukaryotic common ancestor (LECA) (Poole and Gribaldo 2014; Eme et al. 2017).

The rise of bacteria-phagocytosing eukaryotes created a new ecological opportunity for bacteria, as the eukaryotic cytoplasm is a nutrient-rich environment. Many bacteria have adapted to exploit this niche, by resisting digestion once phagocytosed by their predators. Host-adapted lifestyles have evolved many times in many different taxonomic groups (Toft and Andersson 2010), but there are few large groups comprised solely of host-adapted members; such groups include *Legionellales*, *Chlamydiales*, *Rickettsiales*, and *Mycobacteriaceae*. *Legionellales* is a diverse group of *Gammaproteobacteria* (Duron et al. 2018; Graells et al. 2018) that lives only intracellularly and includes the well-studied accidental human pathogens *Coxiella burnetii* and *Legionella* spp. *Legionellales* species vary greatly in lifestyle (Duron et al. 2018), ranging from facultative intracellular (like *Legionella* spp.) to obligate intracellular. The most

Open Access

Article

reduced genomes in *Legionellales* include the vertically inherited *Coxiella* symbionts of ticks (Gottlieb et al. 2015; Guizzo et al. 2017), a louse symbiont in the genus *Legionella* with a 5-fold reduced genome (Rihova et al. 2017), and a protist endosymbiont performing respiration and providing energy to its host (Graf et al. 2021). Because of their rarity and fastidious nature, these host-adapted bacteria are underrepresented in genomic databases; individual isolates from only seven genera have been sequenced out of an estimated >450 genera (Graells et al. 2018).

Hallmarks of adaptation to intracellular space include smaller population sizes, genome reduction and degradation, and pseudogenization (Toft and Andersson 2010). In addition, the infection process linked to an intracellular lifestyle requires a number of specialized functions. For instance, the Type IVB secretion system (T4BSS) plays a key role in the interaction of *Coxiella* (van Schaik et al. 2013) and *Legionella* (Segal et al. 2005; Isberg et al. 2009) with their hosts, injecting a wide diversity of protein effectors into the host cell. These effectors alter the host behavior, preventing the bacterium from being digested and aiding exploitation of host resources, among others. The *Legionella* genus pangenome contains as many as 18 000 different effectors, but only eight of these are conserved throughout the genus (Burstein et al. 2016; Gomez-Valero, Rusniok, et al. 2019).

To better understand the evolutionary history of *Legionellales* and its relationships with their early hosts, we gathered 35 genomic sequences from novel *Legionellales* through whole-genome sequencing, binning of metagenome-assembled genomes (MAGs), and database mining.

Results

Phylogenetic Relationships and Diversity among *Legionellales*

Bayesian and maximum-likelihood phylogenies confirm that *Legionellaceae* and *Coxiellaceae*, hereafter jointly referred as *Legionellales* sensu stricto (ss), are monophyletic, sister clades, and diverged rapidly from each other after the last *Legionellales* common ancestor (LLCA ss) (fig. 1). The phylogeny reveals extensive, previously unknown diversity among *Legionellales* (fig. 1). *Coxiellaceae* comprises two large clades, one including the known genera *Coxiella*, *Rickettsiella*, and *Diplorickettsia*, and the other including the amoebal pathogen *Aquicella* (Santos et al. 2003) and environmental MAGs.

Interestingly, two MAGs (Putative_Legionellales_TARA121 and TARA_PSE_MAG_00004) recovered from the TARA Ocean sampling campaign are included in the *Legionellaceae*, the first one as a sister clade to the *Legionella* genus, and the second clustering within the "green group," having *L. birminghamensis* and *L. quinlivanii* as closest relatives (fig. 1). The discovery of two *Legionella* genomes in a marine environment supports rising evidence that *Legionella* and other genera of the *Legionellales* can colonize saline waters (Gast et al. 2011; Graells et al. 2018).

Two other groups, *Berkiella* spp. and *Piscirickettsia* spp. could not be placed with very high confidence in the tree (supplementary table 1, Supplementary Material online).

However, Bayesian phylogenies (supplementary figs. 1 and 2, Supplementary Material online) inferred with the CAT model consistently placed *Berkiella* as sister clade to *Legionellales* sensu stricto (ss), so *Berkiella* + *Legionellales* is hereafter referred to as *Legionellales* sensu lato (sl). The placement of *Piscirickettsia* is not as consistent, and further studies are needed to establish whether it is more closely related to *Legionellales* or the *Francisella*/*Fangia* group.

Evolution of Genome Sizes

To better understand the evolution of host-adaptation in the order, we inferred ancestral genome sizes from the reconstructed number of protein families (see below), using extant genomes to calibrate the correlation (supplementary fig. 3, Supplementary Material online). As expected from extant genome sizes, *Coxiellaceae* have the smallest genome size average (1.68 Mb), *Aquicella* were intermediate (1.92 Mb), and *Legionella* and *Berkiella* were larger, roughly double as large (3.42 and 3.40 Mb, respectively). Among deep ancestors, the genome size drops between the last free-living ancestor (LFLA, node 107, 2.71 Mb) and the next ancestor (last *Legionellales*/*Piscirickettsia* common ancestor or LLPCA, node 97, 2.16 Mb) toward *Legionellales*, and remains stable in the two subsequent ancestors (LLCA sl, node 96, 2.19 Mb and LLCA ss, node 95, 2.28 Mb). A stable trend is also seen in the *Coxiellaceae*, where the LCA of the family (node 94, 2.09 Mb), and the two daughter nodes (LCA of *Aquicella*, node 93, 2.11 Mb; LCA of *Coxiella*, node 78, 2.05 Mb) have similar genome sizes. In *Legionellaceae*, on the other hand, the trend is toward larger genome sizes (LCA of *Legionellaceae*, node 57, 2.24 Mb; the two subsequent nodes, 56, 2.34 Mb, and especially node 55, 2.98 Mb). The two MAGs branching as sister groups to the *Legionella* genus (TARA_PSE_MAG_00004 and RIFCSPHIGHO2_12_FULL_37_14), have small genomes (2.2 and 1.9 Mb, respectively, see supplementary fig. 2, Supplementary Material online), whereas genomes within *Legionella* (except for "*Ca.* L. polyplacis," an obligate louse endosymbiont; Rihova et al. 2017) range from 2.3 to 4.9 Mb (Gomez-Valero, Rusniok, et al. 2019). The two MAGs branching first on the way to *Legionella* provide some information on how the *Legionella* genus evolved, among others by their small genome size. The first one (TARA_PSE_MAG_00004), branching very shortly after the *Coxiellaceae*/*Legionellaceae* divergence, was reconstructed from a coassembly of 16 metagenomes collected in South-Eastern Pacific by the Tara Ocean expedition (Delmont et al. 2018). Despite its robust phylogenetic association within *Legionellaceae*, its T4BSS resembles *Coxiellaceae*, lacking *icmX*, *icmM/dotJ*, and *icmG/dotF* (supplementary fig. 2, Supplementary Material online). It is also apparently lacking all conserved effectors. The next MAG (RIFCSPHIGHO2_12_FULL_37_14), assembled from groundwater samples taken in the Rifle Aquifer (Colorado), is more similar to *Legionella*. It lacks part of the *icm* operon (*icmP*-*icmB*), probably due to incomplete binning (estimated completeness: 95%), but it harbors the *Legionella*-specific *icmX* and six of the eight conserved *Legionella* effectors. This confirms the view that *icmX* and most of the conserved effectors were gained in the
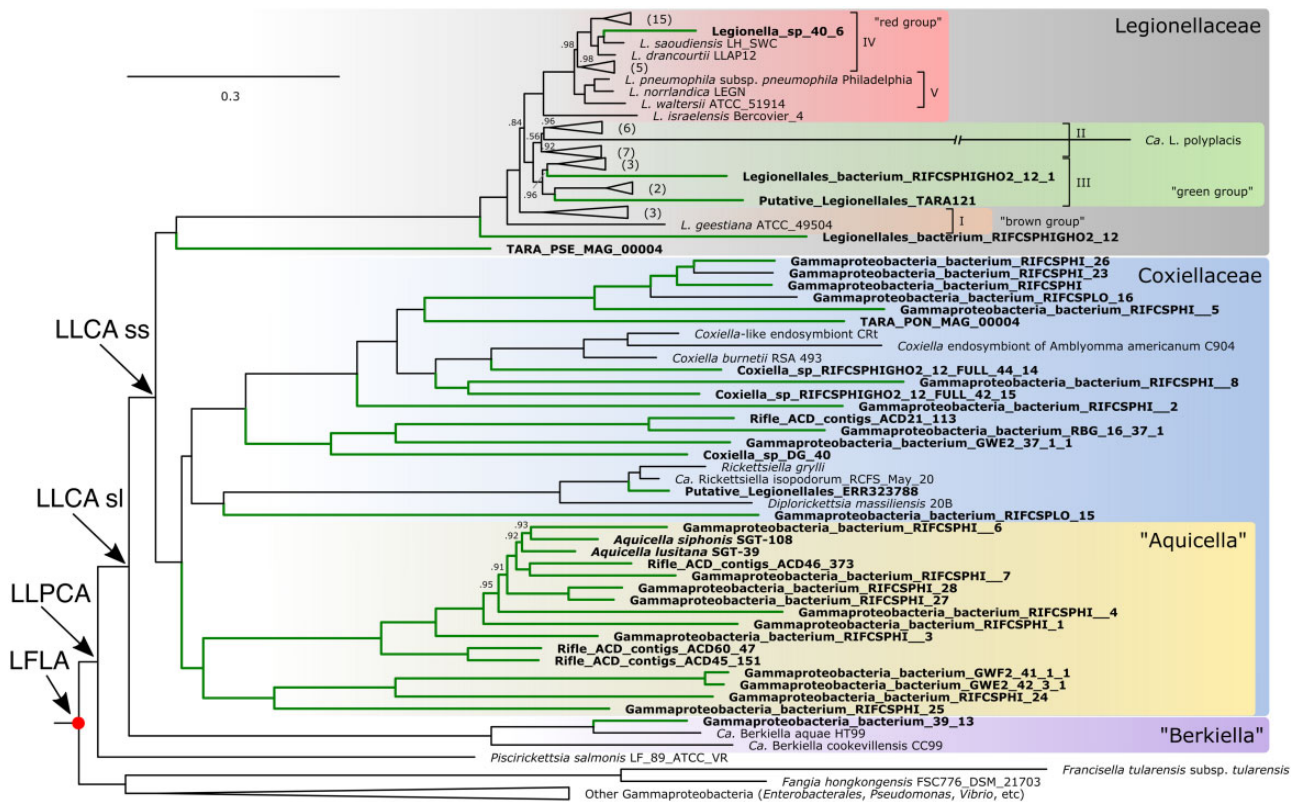
Fig. 1. Bayesian phylogenenetic tree of *Legionellales*. The tree was inferred with PhyloBayes using a GTR+CAT model and a concatenated amino acid alignment of 109 single-copy orthologs (Bact109) comprising 93 *Legionellales* genomes, 16 genomes from other *Gammaproteobacteria*, and rooted with an outgroup of four genomes from non-*Gammaproteobacteria Proteobacteria* (data set Legio93). The tree is a majority-rule consensus tree of all trees across both chains. Numbers on branches show posterior probabilities (pp). Branches without numbers indicate pp = 1. Numbers in parenthesis next to collapsed clades indicate the number of terminal nodes in the clade. Terminal nodes in bold indicate taxa recovered in this study either by database mining or sequencing. Green branches indicate clades with no available genomic data prior to this study. The scale shows the average number of substitutions per site. The colored groups and Roman numerals in *Legionellaceae* correspond to the groupings in Burstein et al. (2016) and Gomez-Valero, Rusniok, et al. (2019), respectively. The LFLA is indicated with a red dot on the tree. LLPCA, last *Legionellales*/*Piscirickettsia* common ancestor; LLCA sl and LLCA ss, last *Legionellales* common ancestor sensu lato (with *Berkiella*) and sensu stricto (without *Berkiella*), respectively. The full tree is available in supplementary figure 1, Supplementary Material online. Size and GC content of all genomes are represented on supplementary figure 2, Supplementary Material online.

Legionellaceae, and not lost by the other groups. It also supports the idea that the genome size increased in the early stage of the *Legionellaceae*.

It should be noted that the size of LFLA (node 107) is probably underestimated. This is caused by the number of protein families which, in turn, tends to be underestimated in very deep nodes. In these nodes, genes are more likely not to be preserved in any of the descendants, due to their scarce representation—in that case the rest of the *Gammaproteobacteria*.

This pattern suggests that the last common ancestor of *Legionellaceae* had a smaller genome than extant *Legionella* species, although it cannot be completely excluded that genome reduction occurred independently in these two MAGs.

Incidentally, both MAGs contained inside the *Legionella* clade III (Gomez-Valero, Rusniok, et al. 2019) also display smaller genomes than their closest relatives: 1.9 and 2.3 Mb, whereas clade III *Legionella* spp. range from 3.1 to 3.9 Mb. The same is also true, albeit to a lesser extent, with the MAG branching in clade IV (Legionella_sp_40_6: 3.1 Mb; rest of the clade: 3.4–4.9 Mb). The reduced genome size in these

MAGs, associated with the longer branches leading to them, might indicate shifts in lifestyles, either toward streamlining as in the *Pelagibacterales* (Giovannoni 2017) or toward an increased dependency on their host (Toft and Andersson 2010), similarly to "*Ca*. Legionella polyplacis" (Rihova et al. 2017). Inferred genome sizes in MAGs may differ from the actual genome sizes, since segments of the genome can be missed by the binning algorithms, and conclusions reached from these should be taken with some caution. However, the MAGs branching within the *Legionellaceae* are predicted to be almost complete, with the least complete being 89% complete and three being >96% complete (supplementary table 2, Supplementary Material online), which supports the results discussed above.

Evolution of Genome Content in the *Legionellales* Last Common Ancestors

To further understand evolutionary paths taken by the ancestors of the order, we reconstructed gene flow within *Legionellales*. The phylogenetic birth-and-death model implemented in Count (Csuros 2010) was used on the same set of

genomes (Legio93) as the tree in figure 1. Count estimates, at each node on the tree, the probability that each gene family is present, present in multiple copies, gained, lost, expanded, and contracted. To analyze specific gene families, we used a 0.5 probability threshold, for each state: for example, we deemed specific families to be gained at a certain node if their probability to be gained was larger than 0.5. However, summary statistics per node (e.g., the total number of families gained on a certain node) are calculated as the sum of gain probabilities for all gene families at that node. These two ways of calculating gains lead to some slight discrepancies when comparing statistics at the node level or specific gene families.

The reconstructed gene flow reveals 553 gene family losses from the LFLA (node 107) to LLCA sl (node 95; fig. 2 and supplementary fig. 2 and table 3, Supplementary Material online), consistent with the decrease in genome size. These 553 losses can be compared with 781 losses on the branch leading to *Fangia/Francisella*, another intracellular group. A subsequent large gain in gene families and in genome size in the last common ancestors of *Legionellaceae* and *Berkiella* spp. (588 and 556 protein families, respectively) but not in the ancestors of *Coxiellaceae* (*Coxiella/Aquicella*) suggests that LLCA had a genome size comparable to that of the latter group (average: 1.78 Mb), compatible with genome sizes of other *Gammaproteobacteria* intracellular bacteria (Toft and Andersson 2010). The details of the gene gains in *Legionellaceae* and *Berkiella* are presented in supplementary results, Supplementary Material online.

Functional analysis of protein family losses from LFLA to the LLCA ss reveals large losses across all COG categories (fig. 3). However, more than half (52.1%) of these protein families are involved in metabolism. The categories that account for the largest decreases include indeed metabolic functions (inorganic ion transport and metabolism [category P], energy production and conversion [C], carbohydrate transport and metabolism [G]) but, maybe more unexpectedly, also functions involved in transcription (K) and signal transduction mechanisms (T).

A closer analysis of the metabolic genes lost from LFLA to LLCA ss reveals a large number of genes directly or indirectly linked to Molybdenum metabolism. Molybdenum (Mo) is a second-row transition metal, the only one essential to most organisms. In most cases, enzymes possessing a Mo atom also contain a cofactor, molybdopterin (Mendel and Bittner 2006). Mo-containing enzymes are essential to catalyze key steps of carbon, nitrogen, and sulfur metabolism (Hille 1996). Among the functions that were lost during transition to intracellular lifestyle in *Legionellales* (LFLA to LLCA), several are linked to Mo metabolism: the molybdopterin synthesis proteins (eight families, including the *moaABCDE* operon and *moeA*), the molybdate transporter operon *modABC* and the molybdopterin-guanine dinucleotide synthase *mobA* are missing from most *Legionellales*. Consistent with Mo being central in sulfur metabolism, several genes of the cysteine metabolism were lost at the same stage (six families, including three transporters), as already noticed for *L. pneumophila* and *Aquicella* spp, both auxotrophic for cysteine (George et al. 1980; Santos et al. 2003). Several other proteins of the sulfur relay system (including thiamine synthesis) are also missing: both subunits of a sulfate adenylyltransferase, *thiS* (immediate sulfur donor in thiazole formation), the sulfurtransferase *tusE*, and *nudJ* (bifunctional thiamine pyrimidine pyrophosphate hydrolase and thiamine pyrophosphate hydrolase). Another group of function predicted to be lost at the same time is nitrite/nitrate metabolism, of which many reactions are catalyzed by Mo-containing enzymes. These missing genes include the *narGHIJKL* operon, encoding among others subunits of the nitrate reductase, a nitrite reductase, and a nitric oxide reductase, as well as two enzymes encoding an allophanate hydrolase. The carbon metabolism-related functions lost at the same stage appear less coherent and seem to include enzymes in various pathways. One exception is the glycogen metabolism operon *glgPACXB* (Chandra et al. 2011). Although it is not possible at this stage to infer the exact order of these losses or their consequences, they form a coherent picture of the LLCA, which became dependent on its host for many of the aspects of sulfur, nitrogen, and carbon metabolism. Interestingly, the recently sequenced "*Ca.* Azoamicus ciliaticola," an obligate endosymbiont of an anaerobic ciliate, harbors many genes involved in denitrification respiration (including *narGHIK*, *modABC*, and the nitrite- and nitrate reductases) predicted to be lost on the immediate descendant of the FLCA. This suggests that "*Ca.* Azoamicus ciliaticola" is only distantly related to *Legionellales*, although a thorough phylogenomic remains to be performed.

Another group of genes lost on the way to intracellular lifestyle are related to protection against oxidizing entities. In *Escherichia coli*, the regulator SoxR senses oxidants and activates other genes that protect the bacterium against superoxide and nitric oxide, among others (Koo et al. 2003). After being activated, SoxR is reduced by the SoxR iron–sulfur cluster reduction factor component, encoded by the operon *rsxACDGE* (Koo et al. 2003). SoxR is missing from the *Legionellales* genomes and *rsxACDGE* is part of the genes lost in the transition to intracellular lifestyle. In *L. pneumophila*, the function of SoxR is replaced by an homolog of OxyR (LeBlanc et al. 2008), widely distributed in the *Gammaproteobacteria*.

Beyond metabolic functions, DNA repair functions are often lost on the path to endosymbiosis (Toft and Andersson 2010). Although the homologous recombination protein gene *recA* is present in the large majority of *Legionellales*, the three genes *recBCD*, which initiate recombinational repair of double-strand breaks in DNA and are known to be missing in *L. pneumophila* (Bryan and Swanson 2011), is shown to be lost right after the LLPCA.

In summary, the deep ancestors of *Legionellales* on the way to LLCA experienced a loss of large portions of central metabolic functions (sulfur, nitrogen, carbon) linked to molybdenum metabolism, and transport of many molecules. This is consistent with these bacteria being adapted to hosts, progressively relying on the latter to provide them with complex molecules.

The flagella, present in the LLCA, is lost in *Coxiellaceae*, consistent with the observation that neither *Coxiella* or *Aquicella* possess one (Santos et al. 2003; Garrity et al.
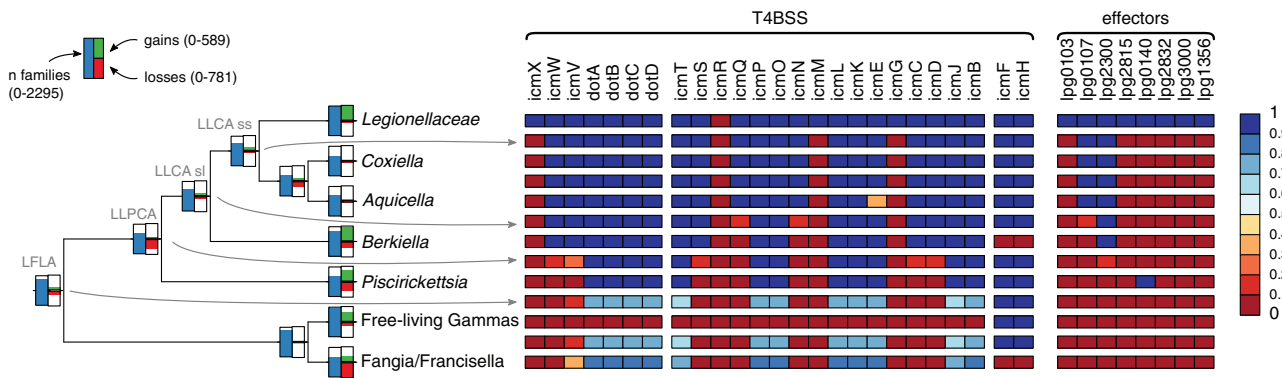
Fig. 2. Overview of ancestral reconstruction of *Legionellales* genomes, with the T4BSS system and the *Legionella*-conserved effectors detailed. The ancestral reconstruction is based on the Bayesian tree in figure 1. At the left of each node, barplots depict the number of gene families (blue, ranging from 0 to 2,295) inferred at that node, as well as the number of gene family gains (green, from 0 to 589) and losses (red, from 0 to 781) on the branches leading to nodes. On the right panel, squares represent genes in the T4BSS—separated according to the three operons present in R64 (Segal et al. 2005)—and the eight effector genes conserved in *Legionella* (Gomez-Valero, Rusniok, et al. 2019). Rows in-between terminal nodes correspond to the last common ancestor of the two nearest terminal nodes, for example, the row between *Aquicella* and *Berkiella* corresponds to the LLCA sl. The color of the squares represents the posterior probability that each protein was present in the ancestor of each group. A complete tree is shown in supplementary figure 2, Supplementary Material online, and the underlying numbers are available in supplementary tables 3 and 4, Supplementary Material online.

Fig. 3. Protein family flow by COG category in the early *Legionellales* ancestors. The upper panels show the absolute number of families present (blue) in the ancestor, lost (red) and gained (green) on the way to its descendant (as indicated on the panel title). The lower panels show the fraction of families lost (red) or gained (green) on the way to the next node, relative to the number of families of that category in the ancestor. COG categories are grouped in four super-categories: information storage and processing (purple), cellular processes and signaling (orange), metabolism (pink), poorly categorized (grey).

2005). Most of the flagellar genes (31 genes, *flgABCDEFGHIJKL, flhABF, fliACDEFGIMNPQRS, motAB, minD*) are predicted to be absent from the last common ancestor of *Coxiellaceae*. The loss of the flagella represents 14.7% of all gene families lost in that ancestor.

Genome Content of the *Legionellaceae* Last Common Ancestors

Whereas the early *Legionellales* ancestors show a net loss of gene families, genome sizes increase in the early *Legionellaceae*. A trend toward larger genomes is unusual in host-adapted bacteria (Toft and Andersson 2010), due, among others, to the progressive loss of exposure to foreign DNA. However, in the case of *Legionella* genus, it appears that genome sizes went from approximately 2.2 Mb in the LLCA ss to approximately 3 Mb in the last common ancestor of genus. We suggest that a supplementary conjugation system (trb) and an improved transformation potential (through the initiation complex of the pilus) might have contributed to this increase. The details are discussed in supplementary results, Supplementary Material online.

Type IV Secretion System

A crucial feature for the success of many host-adapted bacteria is the ability to transfer proteins into the host's cytoplasm, typically through secretion systems. Among the proteobacterial VirB4-family of ssDNA conjugation systems (Type IV Secretion Systems, T4SS), one called T4BSS (also called MPF$_I$ or I-type T4SS) probably arose early in the group (Guglielmini et al. 2013). It is present in almost all extant *Legionellales*, with the exception of the extremely reduced endosymbionts of the group (supplementary fig. 2, Supplementary Material online), where it is either missing completely or pseudogenized. It is partly missing in several of the small, novel *Coxiellaceae* MAGs, possibly indicating increased host dependence. However, it is difficult to assess with certainty whether genes absent in MAGs represent true losses or are the result of incomplete binning of metagenomic contigs. T4BSS in *Legionellales* appears largely collinear (fig. 4 and supplementary fig. 4, Supplementary Material online). Ancestral reconstruction of the order revealed that T4BSS, as it is found in extant *Legionellales*, originated after the LFLA but before the LLCA, with several proteins added over time (fig. 2). IcmW and IcmS (two small acidic cytoplasmic proteins, part of the coupling protein subcomplex; Sutherland et al. 2012; Kwak et al. 2017), IcmC/DotE, IcmD/DotP, and IcmV (three small integral inner membrane proteins, of uncharacterized functions) were gained in the LLCA sl. IcmQ, a cytoplasmic protein and IcmN/DotK, an outer membrane lipoprotein (Ghosal et al. 2019), were acquired in the LLCA ss, after the divergence with *Berkiella*. The limited knowledge about the function of these proteins prevents us to infer exactly how their gain allowed the LLCA to infect eukaryotic cells. However, except for IcmN/DotK, all these proteins are located either in the inner membrane or in the cytoplasm, suggesting that the specific role of the *Legionellales*-gained proteins is related to the coupling protein complex rather than in the

core complex. In *Legionella* however, the T4BSS harbors three specific proteins: IcmX, IcmM/DotJ, and IcmG/DotF. The first one is subject to high recombination rates (Gomez-Valero, Chiner-Oms, et al. 2019), located on the surface of the bacteria, (Khemiri et al. 2008) and thus likely to be exposed to the host. The second one, IcmM/DotJ, is located in the inner membrane, and is a distant paralog of IcmL/DotI with which it forms an heteroduplex (Kuroda et al. 2015). The third one, IcmG/DotF, has a periplasmic part which is thought to be under positive selection (Gomez-Valero, Chiner-Oms, et al. 2019), and is presumably involved in substrate recognition.

The pattern of *Legionellales*-specific T4BSS proteins suggests that the ecological diversity of *Legionellales* and their ability to infect a large spectrum of hosts is linked to an improved way to couple proteins to the secretion apparatus. On the other hand, none of the *Legionella*-specific proteins are cytosolic, and at least one protein is likely to interact with hosts, which is consistent with the even larger host spectrum of *Legionella*.

A homologous T4BSS system is present in *Fangia hongkongensis*, but mostly absent in the free-living *Gammaproteobacteria* and in *Francisella*, a sister clade to *Fangia*. It is likely that the T4BSS in *Fangia* has been acquired by horizontal gene transfer, possibly from *Piscirickettsia* (supplementary figs. 5 and 6, Supplementary Material online). It is however not possible to exclude that a T4BSS was present in the LFLA of *Legionellales*, and subsequently lost on the branch leading to the free-living *Gammaproteobacteria*.

Contrary to T4BSS itself, which is highly conserved throughout the order, effectors are much more versatile. Of the eight effectors conserved in the *Legionella* genus (Gomez-Valero, Rusniok, et al. 2019), only two are found outside of the *Legionellaceae* family (fig. 2): LegA3/AnkH/AnkW (lpg2300), found in *Legionellales* ss and *Berkiella*, and RavC (lpg0107), found in most *Legionellales* ss, but not in *Berkiella*. MavN (lpg2815), which is conserved in *Legionella* spp. and was found in *Rickettsiella* (Burstein et al. 2016), is harbored by a few *Coxiellaceae* species only (fig. 2 and supplementary fig. 2, Supplementary Material online), and is unlikely to have been acquired in the LLCA. The effector LegA3 (lpg2300) contains ankyrin repeats, and has been suggested to play a role in processes involved in modulation of phagosome biogenesis (Habyarimana et al. 2008). The protein translocates to the nucleus, where it interacts with several host targets. It results in changes in host transcription, which promote intracellular bacterial growth (Dwingelo et al. 2019). The function of RavC (lpg0107) is currently unknown, but it is found—beyond *Legionellales*—in *Chlamydiales* (Burstein et al. 2016) and has homologs throughout bacteria. The protein belongs to the required for meiotic division (RMD1) family, characterized in *Saccharomyces cerevisiae* where it is essential for sporulation (Enyenihi and Saunders 2003). It is difficult to draw very specific conclusions based on that level of functional evidence for those two effectors, but their high level of conservation strongly suggests a central role in how *Legionellales* interact with their hosts.
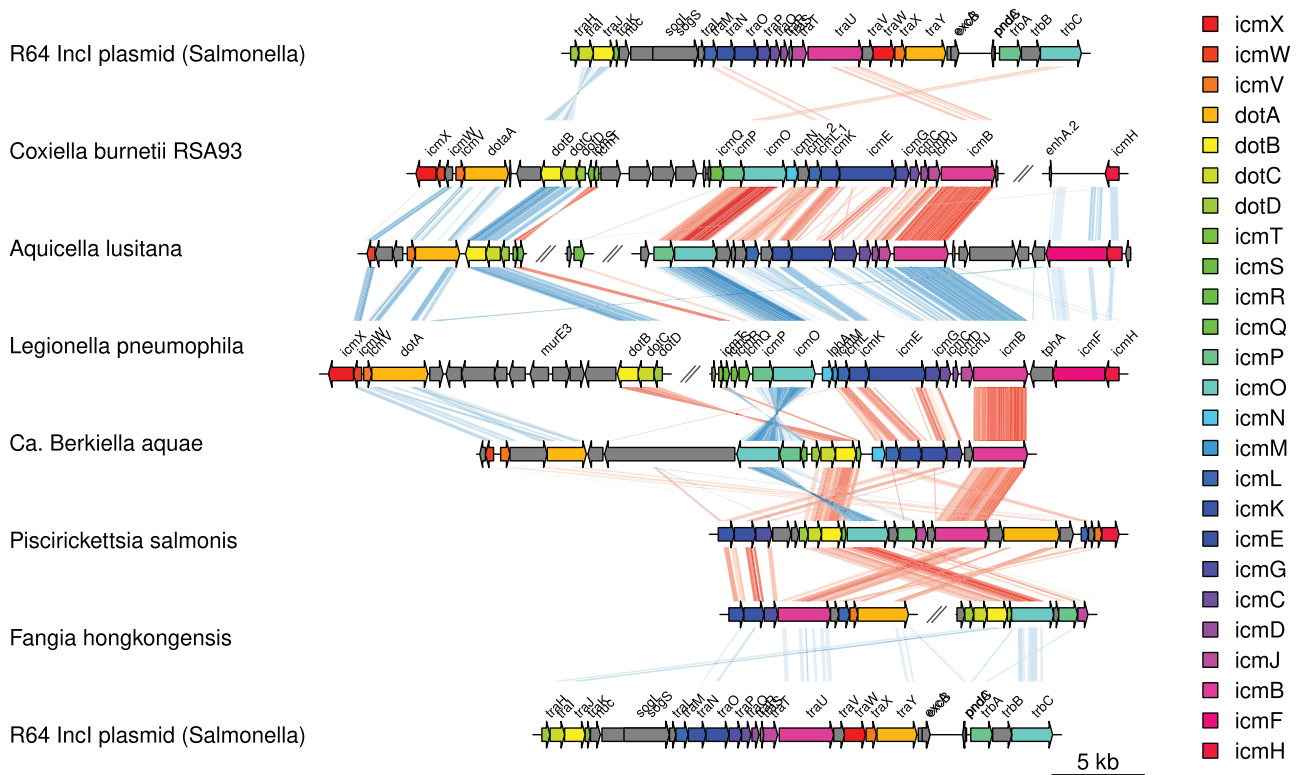
Fig. 4. Collinearity of T4BSS in *Legionellales*. Genes are colored as they appear in *Legionella pneumophila* Philadelphia. Lines connecting rows show similarities between the sequences, as identified by TBlastX. Red lines indicate a direct hit, blue lines a complementary one. Darker shades indicate higher bit scores of the TBlastX hit.

The effector lpg0140 (lpp0155/lpl0140/CetLp1) displays an interesting phylogenetic distribution, being present in all *Legionella* species (except "*Ca.* L. polyplacis"), in one *Coxiellaceae* MAG and in *Piscirickettsia*. Its function is currently unknown, but it shares a homologous domain with the protein LciE, whose expression is induced by the two-component system LciRS, in response to copper stimulation (Linsky et al. 2020). Lpg0140 is specific to *Legionellales* and *Piscirickettsia*, as no homologs could be found outside of these two groups (PSI-BLAST, E-value inclusion threshold $\leq 10^{-5}$; eight rounds until convergence). Further functional studies are required to reveal its role in the infection process of *Legionella* and *Piscirickettsia*.

Dating the Rise of the *Legionellales*

Absolute dating of bacterial trees is often inconclusive, because very few reliable biomarkers can be unambiguously attributed to a bacterial clade and used as calibration points (Brocks and Pearson 2005). However, one such biomarker is okenone, a pigment whose degradation product okenane has been found in the 1.64-Gy-old Barney Creek Formation (Brocks and Schaeffer 2008), and is exclusively produced by a subset of *Chromatiaceae*. *Chromatiaceae* (part of the purple sulfur bacteria) and *Legionellales* are phylogenetically close to each other within *Gammaproteobacteria* (Williams et al. 2010). We reasoned that the divergence of all okenone-producing *Chromatiaceae* from their sister-clade had to be at least as old as the earliest known trace of okenone, that is, ≥ 1.64 Gy (fig. 5). Using this and four other time constraints as well as a relaxed molecular clock model, we were able to

calibrate a maximum-likelihood tree based on a data set including genomes from 105 *Gammaproteobacteria* (of which 25 belong *Legionellales* and 19 to *Chromatiaceae*) and 29 outgroups from a wide diversity of bacteria (Bacteria134 data set). We estimate that LLPCA, the first host-adapted ancestor in the *Legionellales* lineage, existed approximately 1.89 Ga (fig. 5; 95% high posterior density [HPD] 1.75–2.04 Gy), whereas the LFLA of *Legionellales* existed approximately 1.98 Ga (95% HPD 1.84–2.12 Gy). This implies that the host-adaptation event that created *Legionellales* occurred between 2.12 and 1.75 Ga.

We took several steps to mitigate confounding factors in estimating the age of LLCA. These steps are detailed in supplementary results, Supplementary Material online, but briefly: 1) we ensured that the selection of organisms was large, varied, and included a reduced number of fast-evolving organisms; 2) we estimated the effect of the fast-evolving organisms by removing them and estimating the age of the ancestors again; 3) we thoroughly assessed the reliability of okenone as a biomarker, by showing that the genes *crtU* and *crtY*, critical to okenone synthesis in *Chromatiaceae* (Vogl and Bryant 2012), were found almost exclusively in contigs belonging to, or metagenomes containing a sizable fraction of, *Chromatiaceae* and *Actinobacteria*. The latter group does not produce okenone but a different isoprenoid compound using the same genes.

Discussion

The common ability of *Legionellales* bacteria to invade eukaryotic cells combined with the presence and high conservation
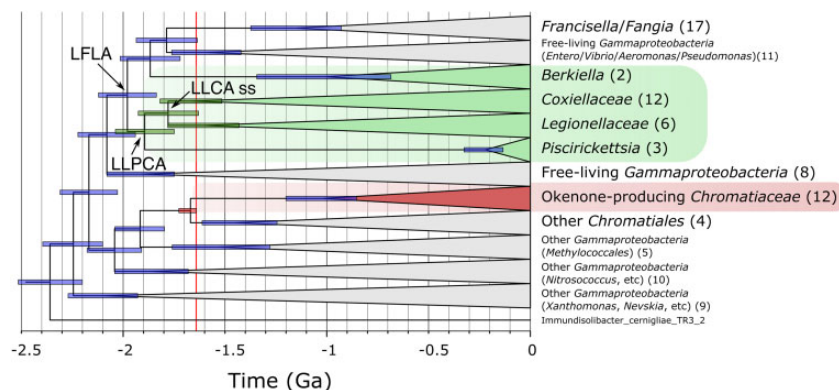
FIG. 5. Bayesian estimation of the appearance of the LLCA. Okenone-producing *Chromatiaceae* are highlighted in red. *Legionellales*, including *Piscirickettsia*, are highlighted in green. The red vertical line is drawn at 1.64 Gy, the age of the Barney Creek Formation which contains okenane, which gives the lower estimate for the divergence of *Chromatiaceae*. Horizontal bars at interior nodes represent the highest posterior density interval (95%) as determined by MCMCtree. The red horizontal bar indicates the divergence of okenone-producing *Chromatiaceae* from their sister group, the green bars indicate ancestors of *Legionellales*, with, from top to bottom, the last common ancestor of *Legionellaceae*, *Legionellales* ss (LLCA ss), *Coxiellaceae*, and the last *Legionellales/Piscirickettsia* common ancestor (LLPCA). The LFLA of *Legionellales* is also indicated. The underlying maximum-likelihood tree is shown in supplementary figure 7, Supplementary Material online and the full tree is shown in supplementary figure 8, Supplementary Material online.

of the crucial host-adaptation genes, namely a complete T4BSS and two effectors, strongly suggest that the last common ancestor of *Legionellales* (LLCA) was already infecting other cells. The hypothesis that LLCA used these mechanisms to infect or interact with other prokaryotes cannot be completely ruled out, but seems extremely unlikely for several reasons. For example, if LLCA was only infecting prokaryotes, then the ability to infect eukaryotes would have to have evolved independently several times within *Legionellales*, in all free-living descending clades, with no exception (all experimentally investigated *Legionellales* are able to live inside the cytoplasm of eukaryotic cells). Furthermore, each of these independent host-adaptation events would have to have involved the same host-adaptation genes (all experimentally investigated *Legionellales* use the same T4BSS to interact with their hosts). Another indication that *Legionellales* were associated with early eukaryotes is provided by the presence of SNARE-like proteins, key to the vesicle fusion process, in the genomes of the former (Neveu et al. 2020). Some of these *Legionellales*-acquired proteins branch deep in the tree, close to root, defined by the homologs belonging to *Heimdallarchaeota* (Neveu et al. 2020), pointing toward a horizontal gene transfer from early eukaryotes to *Legionellales*. This last element of evidence is however mostly circumstantial, since proteins from *Legionellales*, *Heimdallarchaeota*, and eukaryotes were not present on the same tree.

It is also likely that LLCA, like extant *Legionellales*, depended on phagocytosis (or its prototypic version), a mechanism exclusively found in eukaryotes. This implies that LLCA appeared after the division of Archaea and the first eukaryotic common ancestor (FECA), thus placing the rise of phagocytosis and FECA at 1.75 Ga at the latest (lower bound of the 95% HPD for the first host-adapted ancestor, LLPCA), but could be as early as 2.12 Ga (higher bound of the 95% HPD for LFLA). Given a consensual estimate of the age of the LECA of 1.0–1.6 Gy (Eme et al. 2014), the time for

eukaryogenesis, defined as the time elapsed between FECA and LECA (Eme et al. 2017), would be at least 250 My, but could be over 1.1 Gy.

The existence of a phagocytosing eukaryote at 1.89 Gy, likely pre-LECA, has implications for hypotheses of eukaryogenesis. Four of the most prominent of these (reviewed, e.g., in López-García et al. 2017) make different assumptions about the timing of the mitochondrial endosymbiosis. In the hydrogen hypothesis (Martin and Müller 1998), the mitochondria arrived early (mito-early), with the mitochondrial endosymbiosis event itself triggering eukaryogenesis. In the phagocytosing archaeon model (PhAT) (Poole and Neumann 2011; Martijn and Ettema 2013), the syntrophy hypothesis (López-García and Moreira 2006), and the serial endosymbiosis model (Pittis and Gabaldón 2016), the mitochondrion arrive late (mito-late). Specifically, in the PhAT model, phagocytosis machinery is a prerequisite for the fusion of the mitochondrial progenitor with an Asgard archaeon. The very early emergence of phagocytosis proposed in this contribution supports a mito-late scenario. Indeed, the timing of the mitochondrion endosymbiosis has been recently estimated to 1.21–2.053 Gy (Betts et al. 2018). Although confidence intervals overlap, this estimation would place the phagocytosis of the first *Legionellales* (1.75–2.12 Gy, see above) before the mitochondrial endosymbiosis. This timing is also consistent with the mito-intermediate scenario described by Vosseberg et al. (2021). These authors propose that the Asgard-related host that would later acquire the mitochondrion already harbored a certain level of complexity (notably, it had a dynamic cytoskeleton and membrane trafficking), whereas the complex signaling and regulation network and the complex organellar endomembrane system were created after the mitochondrial endosymbiosis. They also suggest that the cytoskeleton and membrane remodeling became increasingly more complex pre-endosymbiosis, perhaps

leading to a primitive phagocytosis system that enabled the mitochondrial endosymbiosis. This primitive phagocytosis system might have been used to engulf the first *Legionellales*.

A recent study estimates LECA to be much older, around 2–2.4 Gy old (Strassert et al. 2021). However, such an old age for LECA heavily relies on one single calibration point, fossil remains found in the approximately 1.6 Gy old Vindhyan formation. These fossils have been interpreted as crown-group red algae, thereby very significantly pushing back the minimum age for LECA. The attribution of these fossils to the crown-group red algae is however not unambiguous, and several authors do not to include it as a calibration point (Betts et al. 2018). Further, the age of LECA in Strassert et al. (2021) is also likely dependent on the prior on the age of the root (3.2–1.6 Gy), the rationale for which is not discussed in the article. These parameters do not significantly affect the main message of the article, which is about the (later) timing of plastid acquisition, but presumably have a significant effect on the estimation of the age of LECA. The latter age should be taken with caution. Should these results however hold true, the conclusions presented here would be different: instead of being coincident with eukaryogenesis, the host-adaptation event that created *Legionellales* would have occurred between LECA and the divergence of Amoebozoa, which are known hosts for *Legionella* and other *Legionellales*.

In summary, we show here that the LLCA already possessed a T4BSS and two effectors, and existed 1.9 Ga. We propose that LLCA, upon being phagocytosed by eukaryotic cells, already had the ability to resist digestion, owing to its host-adaptation genes. Thus, phagocytosis is likely at least 1.9 Gy old, older than previously thought. This hypothesis is consistent with a scenario in which some early eukaryotes developed phagocytic properties and fed on prokaryotes. Some of these, among them LLCA, rapidly acquired the abilities to resist host digestion and exploit the novel, rich ecological niche that is the eukaryotic cytoplasm.

Materials and Methods

Genome Sequencing of *Aquicella* Species
Two species of *Aquicella* (*A. lusitana*, DSM 16500 and *A. siphonis*, DSM 17428) (Santos et al. 2003) were cultivated, sequenced, and annotated as part of this study. The details are available in supplementary methods, Supplementary Material online.

Protein Marker Sets
A set of 139 PFAM protein domains was used as a starting point both to perform quality control of MAGs and for phylogenomic reconstructions. The original set was used by Rinke et al. (2013) (supplementary table 13, Supplementary Material online) to estimate the completeness of their MAGs. We used the same set (referred to as Bact139) to estimate MAG completeness. A large subset of the 139 protein domains is very frequently located in the same protein in a vast majority of Proteobacteria. This was evidenced by investigating 1,083 genomes, using phyloSkeleton 1.1

(Guy 2017) to select one representative per proteobacterial genus and to identify proteins containing the Bact139 domain set. Of these domains which often colocalized in the same protein, only the most widespread one was retained. In total, only 109 domains were used to identify proteins suitable for phylogenomics analysis. This set is referred to as Bact109 and is available in phyloSkeleton 1.1 (Guy 2017).

Metagenomics and Selection of MAGs
The details of the metagenome assembly and binning and of the identification of MAGs belonging to *Legionellales* are available in supplementary methods, Supplementary Material online.

Phylogenomics
Two sets of genomes (Gamma105 and Legio93) were used for phylogenomics in this contribution, and two extra ones (Bacteria134 and Bacteria94, both built on the Gamma105 set) were used only for the time-constrained analysis and are described below. All sets consist of part or all of the novel *Legionellales* MAGs and genomes, supplemented with varying subsets of outgroups. The initial selection of the representative organisms and identification of markers was done with phyloSkeleton 1.1 (Guy 2017), initially choosing one representative per class in the *Betaproteobacteria*, the *Zetaproteobacteria*, and the *Acidithiobacillia*; one per genus in the Gammaproteobacteria, except in the *Piscirickettsiaceae* and the *Francisellaceae* (one per species). That initial selection of genomes was then trimmed down to reduce the computational burden of tree inference.

For both main sets, protein markers from the Bact109 set were identified with phyloSkeleton 1.1 (Guy 2017). Each marker was aligned separately with mafft-linsi v7.273 (Katoh and Standley 2013). The resulting alignments were trimmed with BMGE v1.12 (Criscuolo and Gribaldo 2010), using the BLOSUM30 matrix and the stationary-based trimming algorithm. The alignments were then concatenated. From these alignments, maximum-likelihood trees were reconstructed with FastTreeMP v2.1.10 (Price et al. 2010) using the WAG substitution matrix. Upon visual inspection of the resulting trees, the genome selection was reduced to remove closely related outgroups, and the phylogenomic procedure repeated. Once the genome data set was final, a maximum-likelihood tree was inferred with IQ-TREE v1.6.5 (Nguyen et al. 2015), using the LG (Le and Gascuel 2008) substitution matrix, empirical codon frequencies, four gamma categories, the C60 mixture model (Quang le et al. 2008), and PMSF approximation (Wang et al. 2018); 1,000 ultrafast bootstraps were drawn (Hoang et al. 2018).

The first set of genomes, called Gamma105, was used to correctly place *Legionellales* in *Gammaproteobacteria*, in particular with respect to *Chromatiaceae*. It encompasses 110 genomes, of which 105 are *Gammaproteobacteria*, one is a *Zetaproteobacterium*, three are *Betaproteobacteria*, and one is an *Acidithiobacillia*. The selected *Gammaproteobacteria* include representatives from *Legionellales* (22), *Chromatiaceae* (19), *Francisellaceae* (17), and *Piscirickettsiaceae* (4) (supplementary table 7, Supplementary Material online).

The second set, called Legio93, is focused on *Legionellales* itself and comprises 113 genomes, of which 93 belong to *Legionellales* and the rest to other *Gammaproteobacteria* (16 genomes), *Betaproteobacteria* (two genomes), *Acidithiobacillia* (one genome), and *Zetaproteobacteria* (one genome; supplementary table 2, Supplementary Material online).

For both sets, single-gene maximum-likelihood trees were inferred for each marker. The BMGE-trimmed alignments were used to infer a tree using IQ-TREE 1.6.5, using the automatic model finder (Kalyaanamoorthy et al. 2017), limiting the matrices to be tested to the LG matrix and the C10 and C20 mixture models. Single-gene trees were visually inspected for the presence of very long branches resulting from distant paralogs being chosen by phyloSkeleton.

For both sets, a Bayesian phylogeny was inferred with phylobayes MPI 1.5a (Rodrigue and Lartillot 2014) from the concatenated BMGE-trimmed alignments, using a CAT+GTR model. For the Gamma105 set, four parallel chains were run for 9,500 generations. The chains did not fully converge, but three out of four chains yielded the same overall topology, whereas the last one had the *Piscirickettsia* and the *Berkiella* clades inverted (supplementary table 1, Supplementary Material online). For the Legio93 set, two chains were run for 16,000 generations. The chains converged in an acceptable way and mixed well (maxdiff <0.15, with 3,000 generations as burn-in; ESS >100 for all parameters). The majority-rule tree obtained from the Bayesian trees for Legio93 was subsequently used for the ancestral reconstruction (see below), whereas the one for Gamma105 was used to place *Legionellales* in the *Gammaproteobacteria* and as a ground to build another data set to estimate the time of divergence of the LLCA (see below).

To estimate the date of divergence of *Legionellales*, we created a third data set (Bacteria134), adding 27 additional bacterial genomes from a recent study by Betts (2018) to the Gamma105 data set (containing 110 genomes) (supplementary table 8, Supplementary Material online). Three MAGs from the Gamma105 data set were removed, due to low completeness, yielding a data set with 134 genomes. Protein markers were identified, aligned, and the alignment trimmed as described above. Trimmed alignments were concatenated and the resulting alignment (26,344 sites) was used as input to infer maximum-likelihood with IQ-TREE as described above, but using a C50 mixture model. The resulting tree was used as input to MCMCTree (see below). A fourth data set (Bacteria94) was obtained by 40 removing fast-evolving intracellular organisms (*Legionellales* and *Francisellales*) from the Bacteria134 set and aligning the resulting sequences. The tree based on Bacteria134 was pruned to produce a tree corresponding to the Bacteria94 data set.

Analysis of Genes and Genetic Systems

To relate the earliest documented trace of okenone to a specific ancestor, we investigated literature and searched for homologs of the genes specific to okenone synthesis. We also separately analyzed the genes of the T4BSS, effector proteins, and proteins involved in competence. The details are available in supplementary methods, Supplementary Material online.

Time-Constrained Tree

To estimate the time of divergence of *Legionellales*, we used MCMCTree from the paml package v4.9j (Yang 2007), taking advantage of the implemented approximate likelihood calculations (dos Reis and Yang 2011). The concatenated alignment was considered as a single partition and analyzed under a LG+G model. We assumed a uniform birth/death rate with an uncorrelated clock (clock = 2). Due to the considerable variation in substitution rates existing among bacteria (Kuo and Ochman 2009; Duchêne et al. 2016; Gibson and Eyre-Walker 2019), and as evidenced by the very different branch lengths obtained here (supplementary figs. 9 and 7, Supplementary Material online), a strict clock model was unlikely to be warranted, and therefore not used. A uniform prior calibration distribution was chosen in all cases, with hard bounds. We chose Gy as time unit. The Dirichlet-gamma prior for the mean substitution rate (rgene_gamma) was estimated using the median branch length from tips to root, ($b = 2.55$), and the mean between the minimum (3.21 Gy) and maximum (4.52) age of the root ($t = 3.865$). This provided an estimated substitution rate (b/t) equal to 0.660 substitutions per site per Gy or 6.60×10^{-8} per site per year. In the gamma distribution, the α parameter sets the width of the distribution, and a value of 2 was selected to cover a broad range of substitution rates to account for the fast-evolving organisms in the data set. The β parameter of the distribution was then calculated by setting the middle of the distribution (α/β) to the estimated substitution rate, yielding a β value of 3.03.

To calibrate the clock, it was assumed that the divergence of all okenone-producing *Chromatiaceae* was at least as old as the rocks where the earliest traces of okenane (a degradation product of okenone) was found, $1,640 \pm 30$ Ma old (Page and Sweet 1998; Brocks et al. 2005; Brocks and Schaeffer 2008). The use of a taxonomically broader data set (Bacteria134, see above) allowed to use another four, more distant, calibration points. Divergence time estimates for three of them were taken from the study by Betts et al. (2018) ("Total *Cyanobacteria*," min. age 3,225 Ma, max. age 4,520 Ma; "Crown *Cyanobacteria*," min. age 1,033 Ma, max. age 4,520 Ma; "Crown *Alphaproteobacteria*," min. age 1,033 Ma, max. age 4,520 Ma) and one from a study by Lin et al. (2017) (common ancestor of *Nitrospirae* and *Proteobacteria*, min. age 3,000 Ma, max. age 4,520 Ma).

MCMCTree was run with the concatenated Bacteria134 data set and the maximum-likelihood tree inferred with IQ-TREE as input. Two chains were run for 5 million generations, discarding the first 10% as burn-in. Tracer 1.7.2 (Rambaut et al. 2018) was used to check that both chains had converged (all parameters with ESS >200) and were mixing well. To estimate how the priors affected the runs, parameters obtained from the actual run were compared with those from a run with 1 million generations drawing only from the priors. All parameters displayed very different

distributions, suggesting that the choice of the priors had very little effect on the obtained values.

An analysis of the variation of branch rates was performed to investigate whether a strict clock was indeed not warranted in this case. The coefficient of rate variation (defined as the standard deviation of the branch rates divided by the mean rate) was equal to 0.27, suggesting that the strict clock model could be rejected (Ho et al. 2015).

To estimate whether the increased evolutionary rate in in *Legionellales* and *Francisellaceae* affects the dating of the *Legionellales* divergence, we created a reduced data set (Bacteria94, see above) by removing the intracellular genera *Legionella*, *Francisella*, *Fangia*, and *Piscirickettsia* from the Bacteria134 data set. MCMCTree was run similarly as above, using the maximum-likelihood tree mentioned above, pruned of the relevant clades.

An attempt to estimate the time of divergence of LLCA with BEAST 2 (Bouckaert et al. 2014), using a relaxed clock model (uncorrelated log-normal) (Drummond et al. 2006), was unsuccessful. The chains did not converge, after over 55 million generations.

Protein Family Clustering and Annotation

All 113 proteomes from the Legio93 set were clustered into protein families using OrthoMCL 2.0.9 (Li et al. 2003). All proteins were aligned to each other with the BlastP variant of DIAMOND v0.9.8.109 (Buchfink et al. 2015), with the −more-sensitive option, enabling masking of low-complexity regions (−masking 1), retrieving at most 10^5 target sequences (-k 100,000), with a E-value threshold of 10^{-5} (-e 1e-5), and a precalculated database size (−dbsize 98,280,075). In the clustering step, mcl 14-137 (Enright et al. 2002) was called with the inflation parameter equal to 1.5 (-I 1.5), as recommended by OrthoMCL.

Annotation of the protein families obtained by OrthoMCL was performed by searching for protein accession number in a list of reference genomes (see below). If any protein in a family was present in the first genome, the family was attributed this annotation; else, the second genome was searched for any of the accession numbers, and so on. The reference list was as follows (GenBank accession numbers between parentheses): *Legionella pneumophila* subsp. *pneumophila* strain Philadelphia 1 (AE017354), *Legionella longbeachae* NSW150 (FN650140), *Legionella oakridgensis* ATCC 33761 (CP004006), *Legionella fallonii* LLAP-10 (LN614827), *Legionella hackeliae* (LN681225), *Tatlockia micdadei* ATCC33218 (LN614830), *Coxiella burnetii* RSA 493 (AE016828), *Coxiella* endosymbiont of *Amblyomma americanum* (CP007541), *Escherichia coli* str. K-12 substr. MG1655 (U00096), *Francisella tularensis* subsp. *tularensis* (AJ749949), *Piscirickettsia salmonis* LF-89 = ATCC VR-1361 (CP011849), *Acidithiobacillus ferrivorans* SS3 (CP011849), *Neisseria meningitidis* MC58 (AE002098), *Rickettsiella grylli* (NZ_AAQJ00000000.2). *Legionella* effector orthologous groups were identified by comparing protein accession numbers with the list provided by Burstein et al. (2016). To assign protein families to orthologous groups, eggNOG mapper was used with default settings.

Ancestral Reconstruction

The flow of genes in the order *Legionellales* was analyzed by reconstructing the genomes of the ancestors. The ancestral reconstruction was performed with Count v10.04 (Csuros 2010), which implements a maximum-likelihood phylogenetic birth- and death model. The Bayesian input tree was obtained from the Legio93 data set (see above) and the OrthoMCL families as described above. The rates (gain, loss, and duplication) were first optimized on the OrthoMCL protein families, to allow different rates on all branches. The family size distribution at the root was set to be Poisson. All rates and the edge length were drawn from a single Gamma category, allowing 100 rounds of optimization, with a 0.1 likelihood threshold. Reconstruction of gene flow was then performed by using posterior probabilities.

Supplementary Material

Supplementary data are available at *Molecular Biology and Evolution* online.

Author Contributions

L.G. conceived the study and drafted the manuscript. E.H. performed database screening and metagenomics. A.G. performed the functional analysis. T.A. analyzed the T4BSS and effectors. A.G., E.H., and L.G. performed phylogenomics. All authors contributed to writing the final manuscript and approve it.

Data Availability

The raw and assembled data for the *Aquicella* genomes are deposited at the European Nucleotide Archive (ENA) under study accession number PRJEB29684. The assemblies for *A. lusitana* and *A. siphonis* have the accessions GCA_902459475 (replicons LR699114.1–LR699118.1) and GCA_902459485 (replicons LR699119.1–LR699120.1). MAGs, genomes, associated proteomes, and alignments underlying the trees presented in this contribution are available at Zenodo, with doi:10.5281/zenodo.4607174.

References

Betts HC, Puttick MN, Clark JW, Williams TA, Donoghue PCJ, Pisani D. 2018. Integrated genomic and fossil evidence illuminates life's early evolution and eukaryote origin. *Nat Ecol Evol.* 2(10):1556–1562.

Bouckaert R, Heled J, Kuhnert D, Vaughan T, Wu CH, Xie D, Suchard MA, Rambaut A, Drummond AJ. 2014. BEAST 2: a software platform for Bayesian evolutionary analysis. PLoS Comput Biol. 10(4):e1003537.

Brocks JJ, Love GD, Summons RE, Knoll AH, Logan GA, Bowden SA. 2005. Biomarker evidence for green and purple sulphur bacteria in a stratified Palaeoproterozoic sea. Nature 437(7060):866–870.

Brocks JJ, Pearson A. 2005. Building the biomarker tree of life. Rev Mineral Geochem. 59(1):233–258.

Brocks JJ, Schaeffer P. 2008. Okenane, a biomarker for purple sulfur bacteria (Chromatiaceae), and other new carotenoid derivatives from the 1640 Ma Barney Creek Formation. Geochim Cosmochim Acta. 72(5):1396–1414.

Bryan A, Swanson MS. 2011. Oligonucleotides stimulate genomic alterations of Legionella pneumophila. Mol Microbiol. 80(1):231–247.

Buchfink B, Xie C, Huson DH. 2015. Fast and sensitive protein alignment using DIAMOND. Nat Methods. 12(1):59–60.

Burstein D, Amaro F, Zusman T, Lifshitz Z, Cohen O, Gilbert JA, Pupko T, Shuman HA, Segal G. 2016. Genomic analysis of 38 Legionella species identifies large and diverse effector repertoires. Nat Genet. 48(2):167–175.

Chandra G, Chater KF, Bornemann S. 2011. Unexpected and widespread connections between bacterial glycogen and trehalose metabolism. Microbiology 157(Pt 6):1565–1572.

Criscuolo A, Gribaldo S. 2010. BMGE (Block Mapping and Gathering with Entropy): a new software for selection of phylogenetic informative regions from multiple sequence alignments. BMC Evol Biol. 10:210.

Csuros M. 2010. Count: evolutionary analysis of phylogenetic profiles with parsimony and likelihood. Bioinformatics 26:1910–1912.

Delmont TO, Quince C, Shaiber A, Esen ÖC, Lee ST, Rappé MS, McLellan SL, Lücker S, Eren AM. 2018. Nitrogen-fixing populations of Planctomycetes and Proteobacteria are abundant in surface ocean metagenomes. Nat Microbiol. 3(7):804–813.

dos Reis M, Yang Z. 2011. Approximate likelihood calculation on a phylogeny for Bayesian estimation of divergence times. Mol Biol Evol. 28(7):2161–2172.

Drummond AJ, Ho SYW, Phillips MJ, Rambaut A. 2006. Relaxed phylogenetics and dating with confidence. PLoS Biol. 4(5):e88.

Duchêne S, Holt KE, Weill F-X, Le Hello S, Hawkey J, Edwards DJ, Fourment M, Holmes EC. 2016. Genome-scale rates of evolutionary change in bacteria. Microb Genom. 2(11):e000094.

Duron O, Doublet P, Vavre F, Bouchon D. 2018. The importance of revisiting Legionellales diversity. Trends Parasitol. 34(12):1027–1037.

Dwingelo JV, Chung IYW, Price CT, Li L, Jones S, Cygler M, Kwaik YA. 2019. Interaction of the Ankyrin H core effector of Legionella with the host LARP7 component of the 7SK snRNP complex. mBio. 10:e01942–19.

Eme L, Sharpe SC, Brown MW, Roger AJ. 2014. On the age of eukaryotes: evaluating evidence from fossils and molecular clocks. Cold Spring Harb Perspect Biol. 6:a016139.

Eme L, Spang A, Lombard J, Stairs CW, Ettema TJG. 2017. Archaea and the origin of eukaryotes. Nat Rev Microbiol. 15(12):711–723.

Enright AJ, Van Dongen S, Ouzounis CA. 2002. An efficient algorithm for large-scale detection of protein families. Nucleic Acids Res. 30(7):1575–1584.

Enyenihi AH, Saunders WS. 2003. Large-scale functional genomic analysis of sporulation and meiosis in Saccharomyces cerevisiae. Genetics 163(1):47–54.

Garrity GM, Bell JA, Lilburn T. 2005. Order VI. Legionellales ord. nov. In: Brenner DJ, Krieg NR, Staley JT, Garrity GM, editors. Bergey's manual of systematic bacteriology. 2nd ed. Vol. 2 (The Proteobacteria), part B (The Gammaproteobacteria). New York: Springer. p. 210–248.

Gast RJ, Moran DM, Dennett MR, Wurtsbaugh WA, Amaral-Zettler LA. 2011. Amoebae and Legionella pneumophila in saline environments. J Water Health. 9(1):37–52.

George JR, Pine L, Reeves MW, Harrell WK. 1980. Amino acid requirements of Legionella pneumophila. J Clin Microbiol. 11(3):286–291.

Ghosal D, Jeong KC, Chang Y-W, Gyore J, Teng L, Gardner A, Vogel JP, Jensen GJ. 2019. Molecular architecture, polar targeting and biogenesis of the Legionella Dot/Icm T4SS. Nat Microbiol. 4(7):1173–1182.

Gibson B, Eyre-Walker A. 2019. Investigating evolutionary rate variation in bacteria. J Mol Evol. 87(9–10):317–326.

Giovannoni SJ. 2017. SAR11 bacteria: the most abundant plankton in the oceans. Ann Rev Mar Sci. 9:231–255.

Gomez-Valero L, Chiner-Oms A, Comas I, Buchrieser C. 2019. Evolutionary dissection of the Dot/Icm system based on comparative genomics of 58 Legionella species. Genome Biol Evol. 11(9):2619–2632.

Gomez-Valero L, Rusniok C, Carson D, Mondino S, Pérez-Cobas AE, Rolando M, Pasricha S, Reuter S, Demirtas J, Crumbach J, et al. 2019. More than 18,000 effectors in the Legionella genus genome provide multiple, independent combinations for replication in human cells. Proc Natl Acad Sci U S A. 116(6):2265–2273.

Gottlieb Y, Lalzar I, Klasson L. 2015. Distinctive genome reduction rates revealed by genomic analyses of two Coxiella-like endosymbionts in ticks. Genome Biol Evol. 7(6):1779–1796.

Graells T, Ishak H, Larsson M, Guy L. 2018. The all-intracellular order Legionellales is unexpectedly diverse, globally distributed and lowly abundant. FEMS Microbiol Ecol. 94:fiy185.

Graf JS, Schorn S, Kitzinger K, Ahmerkamp S, Woehle C, Huettel B, Schubert CJ, Kuypers MMM, Milucka J. 2021. Anaerobic endosymbiont generates energy for ciliate host by denitrification. Nature 591(7850):445–446.

Guglielmini J, de la Cruz F, Rocha EP. 2013. Evolution of conjugation and type IV secretion systems. Mol Biol Evol. 30(2):315–331.

Guizzo MG, Parizi LF, Nunes RD, Schama R, Albano RM, Tirloni L, Oldiges DP, Vieira RP, Oliveira WHC, Leite M de S, et al. 2017. A Coxiella mutualist symbiont is essential to the development of Rhipicephalus microplus. Sci Rep. 7:17554.

Guy L. 2017. phyloSkeleton: taxon selection, data retrieval and marker identification for phylogenomics. Bioinformatics 33(8):1230–1232.

Habyarimana F, Al-khodor S, Kalia A, Graham JE, Price CT, Garcia MT, Kwaik YA. 2008. Role for the Ankyrin eukaryotic-like genes of Legionella pneumophila in parasitism of protozoan hosts and human macrophages. Environ Microbiol. 10(6):1460–1474.

Hille R. 1996. The mononuclear molybdenum enzymes. Chem Rev. 96(7):2757–2816.

Ho SYW, Duchêne S, Duchêne D. 2015. Simulating and detecting autocorrelation of molecular evolutionary rates among lineages. Mol Ecol Resour. 15(4):688–696.

Hoang DT, Chernomor O, von Haeseler A, Minh BQ, Vinh LS. 2018. UFBoot2: improving the ultrafast bootstrap approximation. Mol Biol Evol. 35(2):518–522.

Isberg RR, O'Connor TJ, Heidtman M. 2009. The Legionella pneumophila replication vacuole: making a cosy niche inside host cells. Nat Rev Microbiol. 7:12–24.

Kalyaanamoorthy S, Minh BQ, Wong TKF, von Haeseler A, Jermiin LS. 2017. ModelFinder: fast model selection for accurate phylogenetic estimates. Nat Methods. 14(6):587–589.

Katoh K, Standley DM. 2013. MAFFT multiple sequence alignment software version 7: improvements in performance and usability. Mol Biol Evol. 30(4):772–780.

Khemiri A, Galland A, Vaudry D, Chan Tchi Song P, Vaudry H, Jouenne T, Cosette P. 2008. Outer-membrane proteomic maps and surface-exposed proteins of Legionella pneumophila using cellular fractionation and fluorescent labelling. Anal Bioanal Chem. 390(7):1861–1871.

Koo M-S, Lee J-H, Rah S-Y, Yeo W-S, Lee J-W, Lee K-L, Koh Y-S, Kang S-O, Roe J-H. 2003. A reducing system of the superoxide sensor SoxR in Escherichia coli. EMBO J. 22(11):2614–2622.

Kuo C-H, Ochman H. 2009. Inferring clocks when lacking rocks: the variable rates of molecular evolution in bacteria. Biol Direct. 4:35.

Kuroda T, Kubori T, Thanh Bui X, Hyakutake A, Uchida Y, Imada K, Nagai H. 2015. Molecular and structural analysis of Legionella DotI gives insights into an inner membrane complex essential for type IV secretion. Sci Rep. 5:10912.

Kwak M-J, Kim JD, Kim H, Kim C, Bowman JW, Kim S, Joo K, Lee J, Jin KS, Kim Y-G, et al. 2017. Architecture of the type IV coupling protein complex of Legionella pneumophila. Nat Microbiol. 2:17114.

Le SQ, Gascuel O. 2008. An improved general amino acid replacement matrix. Mol Biol Evol. 25(7):1307–1320.

LeBlanc JJ, Brassinga AKC, Ewann F, Davidson RJ, Hoffman PS. 2008. An ortholog of OxyR in *Legionella pneumophila* is expressed postexponentially and negatively regulates the alkyl hydroperoxide reductase (ahpC2D) operon. *J Bacteriol.* 190(10):3444–3455.

Li L, Stoeckert CJ, Roos DS. 2003. OrthoMCL: identification of ortholog groups for eukaryotic genomes. *Genome Res.* 13(9):2178–2189.

Lin W, Paterson GA, Zhu Q, Wang Y, Kopylova E, Li Y, Knight R, Bazylinski DA, Zhu R, Kirschvink JL, et al. 2017. Origin of microbial biomineralization and magnetotaxis during the Archean. *Proc Natl Acad Sci U S A.* 114(9):2171–2176.

Linsky M, Vitkin Y, Segal G. 2020. A novel *Legionella* genomic island encodes a copper-responsive regulatory system and a single Icm/Dot effector protein transcriptionally activated by copper. *mBio* 11(1):11.

López-García P, Eme L, Moreira D. 2017. Symbiosis in eukaryotic evolution. *J Theor Biol.* 434:20–33.

López-García P, Moreira D. 2006. Selective forces for the origin of the eukaryotic nucleus. *Bioessays* 28(5):525–533.

Martijn J, Ettema TJ. 2013. From archaeon to eukaryote: the evolutionary dark ages of the eukaryotic cell. *Biochem Soc Trans.* 41(1):451–457.

Martin W, Müller M. 1998. The hydrogen hypothesis for the first eukaryote. *Nature* 392(6671):37–41.

Martin WF, Tielens AGM, Mentel M, Garg SG, Gould SB. 2017. The physiology of phagocytosis in the context of mitochondrial origin. *Microbiol Mol Biol Rev.* 81:e00008-17.

Mendel RR, Bittner F. 2006. Cell biology of molybdenum. *Biochim Biophys Acta.* 1763(7):621–635.

Neveu E, Khalifeh D, Salamin N, Fasshauer D. 2020. Prototypic SNARE proteins are encoded in the genomes of Heimdallarchaeota, potentially bridging the gap between the prokaryotes and eukaryotes. *Curr Biol.* 30(13):2468–2480.e5.

Nguyen LT, Schmidt HA, von Haeseler A, Minh BQ. 2015. IQ-TREE: a fast and effective stochastic algorithm for estimating maximum-likelihood phylogenies. *Mol Biol Evol.* 32(1):268–274.

Page RW, Sweet IP. 1998. Geochronology of basin phases in the western Mt Isa Inlier, and correlation with the McArthur Basin. *Aust J Earth Sci.* 45(2):219–232.

Pittis AA, Gabaldón T. 2016. Late acquisition of mitochondria by a host with chimaeric prokaryotic ancestry. *Nature* 531(7592):101–104.

Poole AM, Gribaldo S. 2014. Eukaryotic origins: how and when was the mitochondrion acquired? *Cold Spring Harb Perspect Biol.* 6(12):a015990.

Poole AM, Neumann N. 2011. Reconciling an archaeal origin of eukaryotes with engulfment: a biologically plausible update of the Eocyte hypothesis. *Res Microbiol.* 162(1):71–76.

Price MN, Dehal PS, Arkin AP. 2010. FastTree 2 – approximately maximum-likelihood trees for large alignments. *PLoS One* 5(3):e9490.

Quang le S, Gascuel O, Lartillot N. 2008. Empirical profile mixture models for phylogenetic reconstruction. *Bioinformatics* 24(20):2317–2323.

Rambaut A, Drummond AJ, Xie D, Baele G, Suchard MA. 2018. Posterior summarization in Bayesian phylogenetics using Tracer 1.7. *Syst Biol.* 67(5):901–904.

Rihova J, Novakova E, Husnik F, Hypsa V. 2017. *Legionella* becoming a mutualist: adaptive processes shaping the genome of symbiont in the louse *Polyplax serrata*. *Genome Biol Evol.* 9:2946–2957.

Rinke C, Schwientek P, Sczyrba A, Ivanova NN, Anderson IJ, Cheng J-F, Darling A, Malfatti S, Swan BK, Gies EA, et al. 2013. Insights into the phylogeny and coding potential of microbial dark matter. *Nature* 499(7459):431–437.

Rodrigue N, Lartillot N. 2014. Site-heterogeneous mutation-selection models within the PhyloBayes-MPI package. *Bioinformatics* 30(7):1020–1021.

Santos P, Pinhal I, Rainey FA, Empadinhas N, Costa J, Fields B, Benson R, Verissimo A, Da Costa MS. 2003. Gamma-proteobacteria *Aquicella lusitana* gen. nov., sp. nov., and *Aquicella siphonis* sp. nov. infect protozoa and require activated charcoal for growth in laboratory media. *Appl Environ Microbiol.* 69(11):6533–6540.

Segal G, Feldman M, Zusman T. 2005. The Icm/Dot type-IV secretion systems of *Legionella pneumophila* and *Coxiella burnetii*. *FEMS Microbiol Rev.* 29(1):65–81.

Spang A, Saw JH, Jorgensen SL, Zaremba-Niedzwiedzka K, Martijn J, Lind AE, van Eijk R, Schleper C, Guy L, Ettema TJG. 2015. Complex archaea that bridge the gap between prokaryotes and eukaryotes. *Nature* 521(7551):173–179.

Spang A, Stairs CW, Dombrowski N, Eme L, Lombard J, Caceres EF, Greening C, Baker BJ, Ettema TJG. 2019. Proposal of the reverse flow model for the origin of the eukaryotic cell based on comparative analyses of Asgard archaeal metabolism. *Nat Microbiol.* 4(7):1138–1148.

Strassert JFH, Irisarri I, Williams TA, Burki F. 2021. A molecular timescale for eukaryote evolution with implications for the origin of red algal-derived plastids. *Nat Commun.* 12(1):1879.

Sutherland MC, Nguyen TL, Tseng V, Vogel JP. 2012. The *Legionella* IcmSW complex directly interacts with DotL to mediate translocation of adaptor-dependent substrates. *PLoS Pathog.* 8(9):e1002910.

Toft C, Andersson SGE. 2010. Evolutionary microbial genomics: insights into bacterial host adaptation. *Nat Rev Genet.* 11(7):465–475.

van Schaik EJ, Chen C, Mertens K, Weber MM, Samuel JE. 2013. Molecular pathogenesis of the obligate intracellular bacterium *Coxiella burnetii*. *Nat Rev Microbiol.* 11(8):561–573.

Vogl K, Bryant DA. 2012. Biosynthesis of the biomarker okenone: chi-ring formation. *Geobiology* 10(3):205–215.

Vosseberg J, van Hooff JJE, Marcet-Houben M, van Vlimmeren A, van Wijk LM, Gabaldón T, Snel B. 2021. Timing the origin of eukaryotic cellular complexity with ancient duplications. *Nat Ecol Evol.* 5(1):92–100.

Wang HC, Minh BQ, Susko E, Roger AJ. 2018. Modeling site heterogeneity with posterior mean site frequency profiles accelerates accurate phylogenomic estimation. *Syst Biol.* 67(2):216–235.

Williams KP, Gillespie JJ, Sobral BW, Nordberg EK, Snyder EE, Shallom JM, Dickerman AW. 2010. Phylogeny of gammaproteobacteria. *J Bacteriol.* 192(9):2305–2314.

Yang Z. 2007. PAML 4: phylogenetic analysis by maximum likelihood. *Mol Biol Evol.* 24(8):1586–1591.

Zaremba-Niedzwiedzka K, Caceres EF, Saw JH, Backstrom D, Juzokaite L, Vancaester E, Seitz KW, Anantharaman K, Starnawski P, Kjeldsen KU, et al. 2017. Asgard archaea illuminate the origin of eukaryotic cellular complexity. *Nature* 541(7637):353–358.